

Virtual Prototyping of an Automotive Magnetorheological Semi-Active Differential by means of the Reverse Engineering Techniques

A. Lanzotti, F. Renno, M. Russo, R. Russo and M. Terzo

Abstract— Aim of this paper is to describe a research activity on the virtual prototyping, by means of the Reverse Engineering techniques, of an automotive semi-active differential based on the use of a Magneto-Rheological Fluid. The MRF allows to control the locking torque and consequently to improve the vehicle handling. Starting from the 3D digitizing and the virtual reconstruction of a gearbox of a common front wheel drive vehicle, the boundary volume of the new device (MRF LSD) was defined and a preliminary CAD model was realized. Then, optimizing its dimensions and choosing the adequate materials, the final virtual prototype was obtained. The successive GD&T phase allowed to get the best assembly procedure and quality of the final model of the new device. In order to evaluate the goodness of the virtual simulations realized and of the results proposed, a physical prototype was manufactured. Finally, several experimental tests were carried out to validate the design process.

Index Terms—Virtual Prototyping Techniques, Magneto-rheological fluid, Automotive Differential, Reverse Engineering, 3D CAD parametric.

I. INTRODUCTION

The Virtual Prototyping (VP) techniques allow to evaluate the performances of a new product through multiphysics simulations before its manufacturing. The virtual prototype is a geometrical model completed by the physical properties useful for the engineering analyses to be carried out. They help reduce the cost and the time to market of the new products, avoid errors, and improve the quality of the results. [1 – 2]

VP can be very useful to study human machine interactions. A real human can interact with a virtual

A. Lanzotti is with the Dipartimento di Ingegneria Industriale, Università degli Studi di Napoli Federico II, Napoli, 80125 ITALY (e-mail: antonio.lanzotti@unina.it).

F. Renno is with the Dipartimento di Ingegneria Industriale, Università degli Studi di Napoli Federico II, Napoli, 80125 ITALY (e-mail: fabrizio.renno@unina.it).

M. Russo is with the Dipartimento di Ingegneria Industriale, Università degli Studi di Napoli Federico II, Napoli, 80125 ITALY (e-mail: michele.russo@unina.it).

R. Russo is with the Dipartimento di Ingegneria Industriale, Università degli Studi di Napoli Federico II, Napoli, 80125 ITALY (e-mail: riccardo.russo@unina.it).

M. Terzo is with the Dipartimento di Ingegneria Industriale, Università degli Studi di Napoli Federico II, Napoli, 80125 ITALY, (corresponding author, phone: +390817683277; fax: +390812394165; e-mail: m.terzo@unina.it).

prototype thanks to virtual and augmented reality technologies [3 – 5]. In [6] the feasibility of the assembly operations of all the parts inside the tokamak (device for the production of the controlled thermonuclear fusion power), by means of the combination of VP and VR techniques, is analysed.

Furthermore, the VP can be very useful to investigate on the interaction of multiple physical models. So, a multiphysics approach is mandatory to understand real physical phenomena in order to develop and design efficient and safe products. An example can be provided by the study of the interactions between electromagnetic (EM) loads and structures. For this reason VP is becoming fundamental in the nuclear fusion field [7]. In [8] its advantages for the development of the nuclear fusion plants and their devices are showed. Another example is given by the study of the interaction between EM fields and magnetorheological materials. The peculiarities of the change of the behaviour of the Magnetorheological fluids (MRF) varying the properties of the magnetic field applied are very interesting to design and develop a new mechanism. For this reason the use of the MRF became very common and remarkable in several application fields [9 – 12].

Finally, the integration of VP and Reverse Engineering techniques is useful when the new product is an evolution of a previous one and has to fulfil functional and geometrical system constraints. It happens when a new subsystem part of a complex system has to be designed. Being a real object, i.e. the old part, available in the system by means of contact or contactless systems, it is possible to define the constraints or shape of the new digital model. RE techniques are also deeply used in many fields like: industrial (automotive, aerospace, manufacturing), computer graphics (simulations, videogames), archaeological and biomedical [13 – 14]. The result of a Reverse Engineering process can provide the virtual prototype of the starting model. Then, it has to be optimized considering the requirements and the constraints of the project ideated. Otherwise, the result can be the clone of the starting model due to the constraints defined by the shapes and dimensions imposed by a specific design [13].

II. TARGETS

This paper focuses on the virtual prototyping of a controllable limited slip differential. The main aspect of this new device is the use of a contactless clutch activated by

means of the magnetization of a Magneto-Rheological (MR) fluid and, consequently, no hydraulic pump or electric motor are needed. MR fluid is extensively used in brake, clutch and damper [15 – 17], but no examples concerning the design and the development of a MR fluid based automotive differential are available in the scientific literature. So, four main targets are pursued and described in the paper:

- The 3D reconstruction, by means of the Reverse Engineering techniques, of the differential housing to define the available space for the new device in a front wheel drive vehicle;
- The definition of the geometrical design constraints in terms of shape and maximum dimensions;
- The design of the concept that satisfies the geometrical constraints previously defined for the selected architecture;
- The making of the optimized virtual prototype of an innovative semi-active device that transfers and biases the torque between the two half-shafts by means of the magnetization of a MR fluid.

So, the design of the Magneto-Rheological Fluid Limited Slip Differential (MRF LSD) started from the constraints imposed by the available space that in origin was occupied by a passive device (free differential) located in the gearbox of a common Front Wheel Drive (FWD) vehicle: this represents a strict design challenge caused by the complexity of the chosen power train layout.

Therefore, a RE process based on 3D laser scanner measurements was adopted to firstly determine the boundary volume and to delineate the maximum external sizes of the MRF LSD. After the 3D reconstruction of the models of the gearbox and of the gearbox cover, the appropriate MRF LSD architecture was defined and a preliminary virtual prototype was obtained according to the Top-Down modeling to satisfy the geometrical set constraints previously identified. Then, once the materials were chosen and the dimensions optimized, the final CAD model was realized according to the quality requirements set by means of the Design For Assembly (DFA) and of the Geometric Dimensioning and Tolerancing (GD&T) procedures. The successive manufacturing phase allowed to realize the physical prototype that was then tested in order to verify its locking effect.

The experimental results have highlighted the functionality of the MRF LSD and validated the design process used.

The section III of the paper analyses the MRF LSD working principle, section IV describes the virtual prototyping techniques used, with particular attention to the Reverse Engineering processes, whereas the results of the physical prototyping and of the first tests are showed in section V.

III. MAGNETORHEOLOGICAL FLUID LIMITED SLIP DIFFERENTIAL

The gearbox coupled with the engine by means of a clutch and differentials commonly make up the vehicle drive-line. The need to transmit the torque to the driving wheels and, at the same time, to make the wheels free to

rotate at different speed, make the differential very functional for the purpose. The differential (called free or open differential) commonly used receives the torque from the gearbox and splits it into two equal parts that act on the driving wheels. Consequently, neglecting the internal friction loss, the driving wheels are subjected to the same driving torque and can rotate at different speed in accordance with the vehicle kinematics. In order to solve the limit of the free differential several developments were carried out. If one of the driving wheel travels on a low friction surface, the tyre-road interaction force is minimized and a limited torque is transmitted to the other one so the vehicle is unable to start. Suitable passive devices [18] (so called limited slip differentials) were realized in order to transmit the torque to a wheel even if the other one is on a slippery surface. In the limited slip differentials the two side gears are mated and generate different driving torques. This differential locking effect makes the vehicle capable to move also in presence of a wheel characterized by low traction. The locking torque that characterizes the limited slip differentials is typically depending on the wheel relative speed or on the torque acting on the differential case and generates its effects independently from the vehicle handling, e.g. understeering/oversteering. Consequently, in some dynamic conditions, the locking torque can also determine an undesired behaviour of the vehicle. Thanks to the development of the electronic control, semi-active and active differentials were realized: these devices are characterized by a controllable locking torque and typically use hydraulic or electrical actuation systems to engage a clutch which determines problems in terms of wear and NVH (Noise, Vibration and Harshness) due to the sliding between the parts that are in contact.

A. Magnetorheological fluids

Magnetorheological (MR) fluids are suspensions of micrometer-sized and magnetisable particles in a carrier fluid. Normally, MR fluids are free-flowing liquids, having a consistency similar to that of a lubricant oil. However, when a magnetic field is applied, their rheology turns into a more solid-like gel. MR fluid rheology is modelled in pre-yield and post-yield regimes. In the pre-yield regime, MR fluids show a visco-elastic behaviour. As for visco-elastic materials, while some of the energy applied is recovered (elastic behaviour), some is dissipated in the form of heat. The visco-elastic behaviour of the MR fluids in the pre-yield regime is analyzed by linear visco-elastic theories. On the other hand, the MR fluid post-yield behaviour in presence of a magnetic field is approximated by the Bingham plastic model [19].

$$\tau = \tau_{yd}(H) + \eta \frac{d\gamma}{dt} \quad (1)$$

where, τ is the shear stress, τ_{yd} is the dynamic yield stress due to the applied magnetic field (H), η is the no-field fluid viscosity, and $d\gamma/dt$ is the shear rate. When the magnetic field intensity rises, the ferromagnetic particles find an orientation and the yield stress increases. This property makes the MR fluids functional for the employment in controllable devices [20 – 23].

B. Analysis of the MRF LSD

Fig. 1 illustrates the MRF LSD logical scheme. It consists of a conventional part and an unconventional one. The side gears (A and B), the planetary gears (G), the differential case (P) and the differential gear (R) characterize the conventional part of the MRF LSD. The unconventional part consists of a disk housing (C) and a coil (S). The disk housing engages the side gear A and the differential case P, and contains facing plates, alternately integral with the side gear and the differential case P, that perform the friction surfaces. Suitable spacer elements create a gap in which the MR fluid is contained.

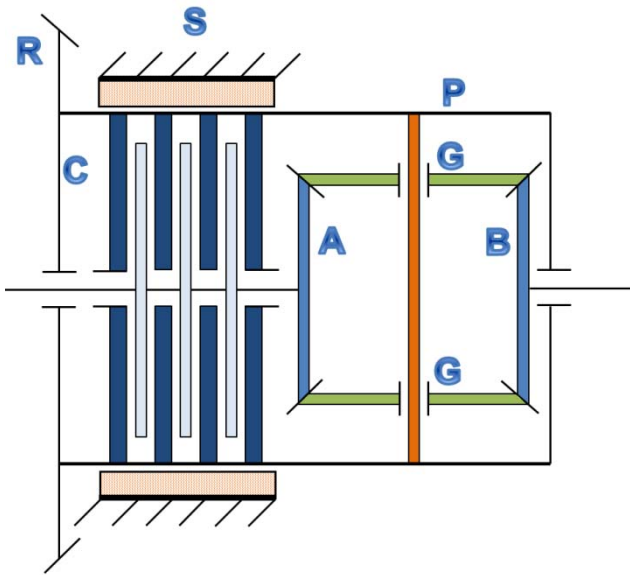


Fig. 1. Logical scheme of the MRF LSD.

The device is able to transfer the power to the driving wheels and, changing the coil current, it is possible to bias the torque with a different ratio. Whereas in a passive limited slip differential the locking torque depends on the relative sliding or on the torque acting on the differential case, in the MRF LSD it essentially depends on the magnetic field.

IV. DESIGN OF THE MRF LSD

A. Procedure

The advantages offered by the CAE techniques allow the optimization of the final prototype since the starting design phases. The main target for the case studied is to predict as soon as possible the variation of the magnetic field generated during the functioning so to improve the performances of the device, and also to reduce the design errors. Therefore, the CAD modeling of the MRF LSD by means of a 3D parametric software was needed to manufacture its physical prototype. Consequently, an electromagnetic finite element analysis was realized to get the best results.

The design of the MRF LSD started from a concept generated following the procedure reported in Fig. 2, considering the gearbox of a common front wheel drive vehicle equipped with a free differential.

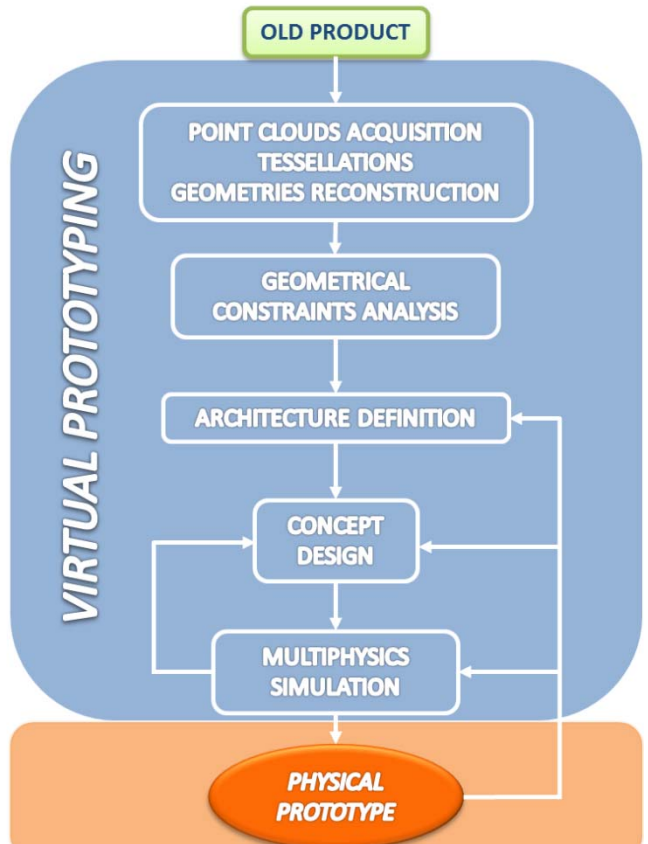


Fig. 2. Procedure followed for the realization of the physical model of the MRF LSD.

The first step was to conceive the starting concept of the MRF LSD according to the working principle required. Then, the shape and the dimensions of the gearbox were digitized by means of a RE process and used as constraints to realize the preliminary CAD model of the device. All the CAD parts were created starting from it. At the end of this phase, as a wrong choice could worsen the magnetic efficiency, the materials were opportunely selected and applied to the preliminary CAD model for the successive simulations to define the properties of the magnetic field and to have the full control of the behaviour of the device. So, after this step it was possible to determine the optimal dimensions for the improvement of the performances of the device. It allowed to get the final CAD model.

Next step was the use of the GD&T methods to manufacture the physical prototype according to the accuracy and the economic requirements. So, the drawings of each element of the device were realized in order to use the typical CAM techniques. Once the physical prototype was manufactured (Fig. 11), several experimental tests were carried out to evaluate the good functioning of the MRF LSD and the goodness of the simulations done.

B. Reverse Engineering – Requisites and Constraints

Aim of this phase was the definition of the shape and dimensions of the carter, with particular attention to its internal sizes to be used as starting geometrical and dimensional constraints for the design of the MRF LSD. To reach this target a Reverse Engineering (RE) process was adopted.

The RE techniques are useful to obtain the virtual prototype of a physical object when its original CAD model is not available. It can be modifiable, after the adequate reconstruction and feature recognition phases, or simply used for visualization or analysis purposes [13].

A typical RE procedure starts with the acquisition done by means of contact or contactless systems in order to get a dense points cloud that represents the outer shape of the object. The first, as the CMM (Coordinate Measuring Machines), are the industrial standards for the tolerance control due to their high measurement precision. Otherwise, if it is not strictly required, the contactless systems, i.e. based on optical principles like laser scanners, could be more suitable due to their acquisition speed and to their costs [13].

For the design of the MRF LSD, the predictable accuracy of a common laser scanner system was assumed acceptable and so the Konica Minolta 9i laser scanner, available at IDEAS Laboratory at University of Naples [24], was used (about ± 0.05 mm in the XYZ direction). Typically, the acquisition of a 3D real object by means of an optical system is troubled by occlusions problems and/or noises caused by incorrect settings of the ambient (lights, reflective surfaces, inappropriate distance between the laser scanner and the object). So, many scans around the gearbox in a dark room were realized using an adequate reference system to allow the right and easy merging phase of the point clouds. Furthermore, because of the high reflectivity of the object material (steel), it was beforehand dazzled with a particular powder to make its surfaces opaque and to avoid unwanted problems due to the laser beam. After editing the final points cloud to reduce the noise and the errors of the acquisition, and after the successive tessellation, the surfaces of the gearbox and of its cover were obtained.

The main difficulties of this step were related to the reconstruction in the virtual environment of the many peculiarities of the original models. In particular, as the gearbox is characterized by many cut-outs, freeform shapes, ribs and holes, the 3D acquisition and the editing of the point clouds were difficult and took a long time.

Then, starting from the point clouds edited and optimized, it was possible to carry out the surface fitting. The results of this phase for the gearbox and the gearbox cover, obtained in *Geomagic Studio Environment* (RE dedicated software), are showed in Fig. 3.

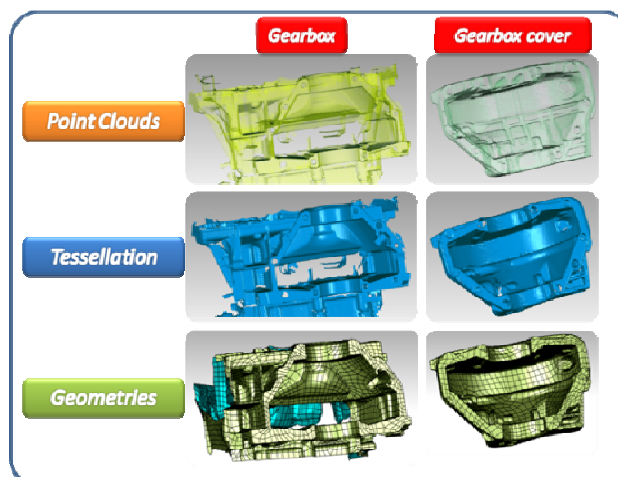


Fig. 3. Reverse Engineering phases of the Gearbox and of the Gearbox cover

Then, the reconstruction of the CAD models (Figures 4, 5 and 6) was followed according to the Reverse Engineering procedures.

In fact, starting from the geometries showed in Fig. 3 the feature recognition phase was possible. The work done during the editing operations was essential to avoid unwanted errors. The better the surfaces the better the results.

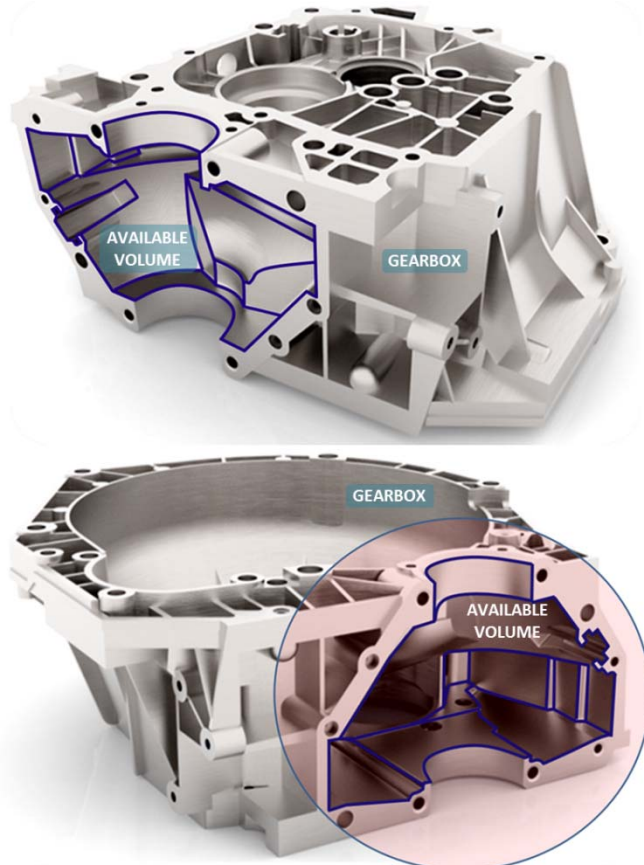


Fig. 4. Result of the CAD model reconstruction of the gearbox by means of the RE techniques and volume available for the design of the MRF LSD.

In particular, in this phase, several geometric entities (points, lines, planes, circles, cylinders) were used to identify the features corresponding to the elements acquired and reconstructed during the previous steps. So, the creation of all the CAD entities such as the rounds, the fillets, the holes, and the many features acquired of the two mock-ups, was possible. The definition of the available volume for the design of the MRF LSD was possible (Fig. 4 and Fig. 5). Therefore, the final reconstructed CAD models of the elements of the gearbox (Fig. 4) and of the gearbox cover (Fig. 5 and Fig. 6) are showed.

C. Configuration of the MRF LSD

Firstly, the definition of the layout of the device was necessary. The main elements of the MRF LSD are: the Differential case, the Side and Planetary gears, the Disk housing and the Differential Gear. Each part has to be opportunely placed to respect the dimensional requirements to optimize the magnetic flow and to improve the performances of the device. Two layouts were analyzed considering the position of the Differential Gear imposed by the pinion.



Fig. 5. Result of the CAD model reconstruction of the gearbox cover by means of the RE techniques and available volume for the design of the MRF LSD.



Fig. 6. Result of the CAD model reconstruction of the gearbox cover by means of the RE techniques.

The first, similar to the case of an open differential with the addition of the disk housing, is based on the following displacement: Differential gear, Side and Planetary Gears and Disk Housing. The second inverts the position of the last two elements.

Due to the available space and as the disks with bigger diameter allowed to reduce the current needed, the second layout was chosen (Fig. 7).

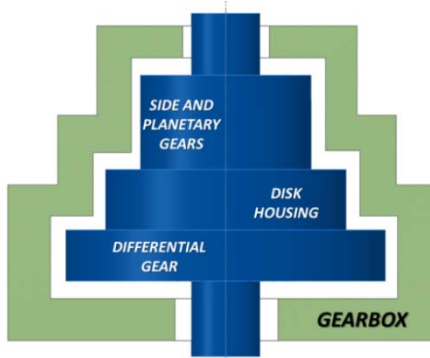


Fig. 7. Layout chosen for the design of the MRF LSD.

D. CAD modeling

Preliminary CAD model

The virtual model of a complex real prototype can be realized following two approaches: *Bottom-Up* or *Top-Down*. The first contemplates the preliminary modeling of each single part and their successive assembly. This procedure is suggested for a not high number of parts. The main drawback is that the attention of the designer is

focused on only one part at a time and he doesn't consider all the other elements and their interdependences. So, if there are wrong dimensions or if several modeling mistakes happen, a successive analysis and correction phase is needed. Instead, by means of a *Top-Down* approach, he preliminarily defines a set of datum elements (points, axes and planes) used as a main reference system for the whole assembly and its subassemblies and parts, making each update and modification easier. So, the shape of each single part is delineated by means of its external sizes and then it is detailed, avoiding in real time the modeling errors like unwanted contacts, interferences or clearances between the parts. In this way, the designer has a complete view of the single parts inside the assembly and furthermore he can verify every its functional aspect. This approach is recommended for the large dimensions assemblies modeling [25].

As the CAD model of the MRF LSD has to be inserted in a carter of an existing vehicle as mentioned in par. 4.1, a *Top-Down* approach was adopted according to the shape and the dimensions acquired by means of the RE process. The first step was to import the results of the reconstruction process into the CAD environment. Then, according to the 3D CAD parametric modeling techniques, the internal surfaces of the RE models of the gearbox and of its cover were used for the definition of seven planes that represented the limits for the MRF LSD in the main directions.

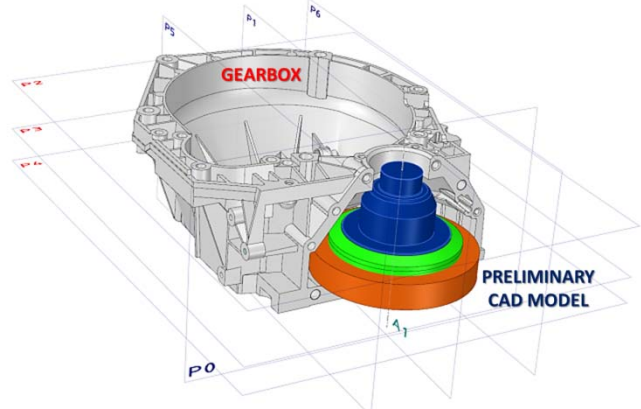


Fig. 8. Reconstructed model of the differential housing and datum planes used for the design of the preliminary CAD model of the MRF LSD according to the *Top-Down* approach.

The A1 rotation axis of the MRF LSD was defined as intersection between the P0 and P1 planes. The limit for the top part of the differential case was the P2 plane whereas the P3 was the limit for the inferior part of the coil housing. The P4 plane defined the boundaries for the bottom part of the differential gear. The maximum diameter of the differential gear was defined by the P5 and P6 planes. Starting from these datum and from the layout showed in Fig. 7, the preliminary CAD model was created (Fig. 8).

Furthermore, the definition of the materials and the optimization of the dimensions of the device were needed to obtain and detail the final CAD model of the MRF LSD according to the magnetic field requisites (Fig. 10). The selection of the material of each part is an important step in the design of the MRF LSD. In fact, each material is characterized by the magnetic permeability, i.e. the aptitude of the material to be crossed by the magnetic flux and so to

modify the efficiency of the magnetic field. Therefore, specific choices concerned the materials (Table 1) in the manufacturing phase of the MRF LSD. Considering the costs, the permeability and the manufacturability, low carbon steel (AISI 1008) was selected for the components of the magnetic circuit, i.e. the cores and disks (Fig. 10). Instead, for the non-magnetic parts, AISI 304 was chosen.

The selection of the controllable MR fluid was realized starting from the analysis of the commercially available products. In particular, the following characteristics were considered:

- High sensitivity of the MR fluid to the applied magnetic field (B-H curve);
- Low hysteretic behaviour;
- Broad operating temperature range;
- No-field viscosity.

Considering the previous properties, the MRF – 140CG®, by Lord Corporation, was chosen. Its characteristics are listed in Table I.

Table I. MRF Properties of MRF – 140CG®

| Properties | Value/Limits |
|------------------------------|-------------------------|
| Base fluid | Hydrocarbon |
| Operating temperature | -40 °C to 130 °C |
| Density range | 3.54 to 3.74 g/cm³ |
| Colour | Dark grey |
| Weight percent solids | 85.44% |
| Specific heat at 25 °C | 0.71 J/g°C |
| Thermal conductivity at 25°C | 0.28 – 1.28 W/m°C |
| Viscosity at 40°C | 0.28 (\pm 0.07) Pa s |

E. Design for assembly and MRF LSD final CAD model

Lastly, the final configuration of each component of the MRF LSD was defined according to the magnetic requisites and to the Top-Down modeling approach.

In particular, the Design For Assembly (DFA) procedures were adopted to optimize the virtual prototyping phase of the MRF LSD and to improve the quality of the results. They allow to simplify and improve the realization of a product taking into account from the beginning the assembly operations of the parts of the final model [26]. So, the first steps were the identification of the main components of the MRF LSD and the minimization of the number of parts to create and then to assemble. Afterwards, the definition of a hierarchical structure was needed to organize the product at different levels characterized by decreasing complexity. The Fig. 9 shows the levels of the hierarchical structure used to design and then to assemble the final product according to the Top-Down procedure described in the previous paragraph.

So, the final CAD model of the MRF LSD consists of two main subassemblies: 1) the Planetary Gears Housing, 2) the Magneto-Rheological Fluid brake. The first contains the gears, that allow to differentiate the velocity of the car wheels during the curve, and their Differential case. The Magneto-Rheological Fluid brake includes two different subassemblies: the Coil Housing and the Disk housing. In the first there are the bobbins used for the magnetic circuit. The second contains several plates soaked in the MRF.

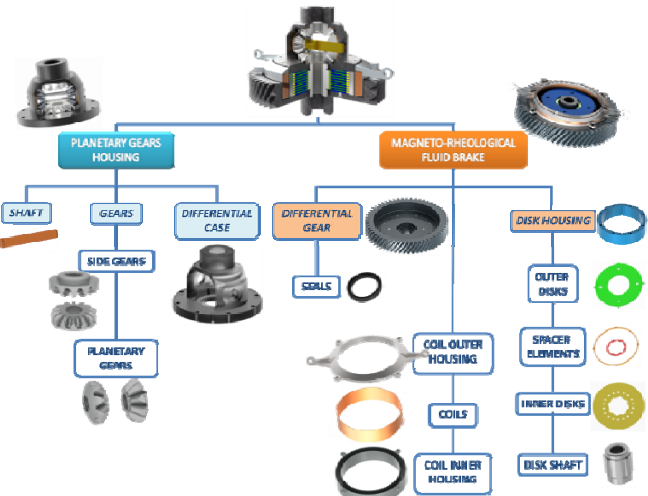


Fig. 9. Hierarchical structure of the CAD assembly of the MRF LSD.

During the functioning of the device the coil housing is fixed while the disk box rotates, with an assigned torque, together with the Differential gear and the Differential case.

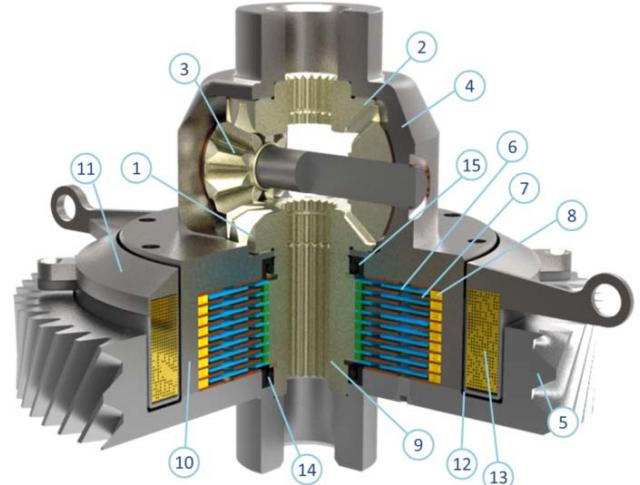


Fig. 10. MRF LSD section.

All the components of the MRF LSD assembly and their chosen materials are listed In Table II.

Table II. Components of the MRF LSD

| S/No | Description | Material |
|------|--------------------|---------------------------------------|
| 1 | Side gear A | Standard steel |
| 2 | Side gear B | Standard steel |
| 3 | Planetary gear | Standard steel |
| 4 | Differential case | Low carbon steel (AISI 1008) |
| 5 | Differential gear | Low carbon steel (AISI 1008) |
| 6 | Inner disk | Low carbon steel (AISI 1008) |
| 7 | Outer disk | Low carbon steel (AISI 1008) |
| 8 | Spacer elements | Austenitic stainless steel (AISI 304) |
| 9 | Disk shaft | Austenitic stainless steel (AISI 304) |
| 10 | Disk housing | Austenitic stainless steel (AISI 304) |
| 11 | Coil outer housing | Low carbon steel (AISI 1008) |
| 12 | Coil inner housing | Austenitic stainless steel (AISI 304) |
| 13 | Coil | Copper |
| 14 | Sealing | Steel |
| 15 | Sealing | Steel |

Furthermore, the Fig. 11 shows the final model of the MRF LSD inside the Differential Housing digitized and reconstructed by means of the RE techniques described before.



Fig. 11. Result of the CAD model reconstruction of the differential housing together with the virtual prototype of the MRF LSD.

F. FEM Analyses

Typical stress and fatigue analyses to obtain the best configuration of the MRF LSD were realized separately on the components that hold up mostly the loads i.e. the differential case, the disk housing and the differential gear. The other parts of the new device, including also the teeth of the differential gear, were not analysed because they were not different from the typical elements according to the standards [27 – 28]. The components were designed taking into account a loading condition produced by an engine torque of 200 Nm on the differential gear, amplified by means of a high gear ratio of the transmission (i.e. 16). So, because of the helical teeth gearing, the loading forces that cause the wanted torque were tangentially applied on the surface created on the base circle of the differential gear and that subtends two of the teeth (Fig. 12).

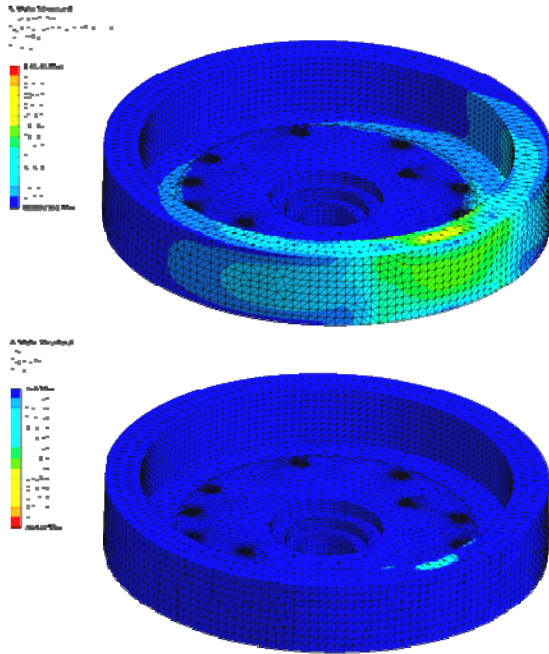


Fig. 12. Result of the stress and fatigue analyses on the differential gear.

The analysis of the differential case was realized fixing it in correspondence of the two holes at the top and applying the torque to the bottom surface (Fig. 13).

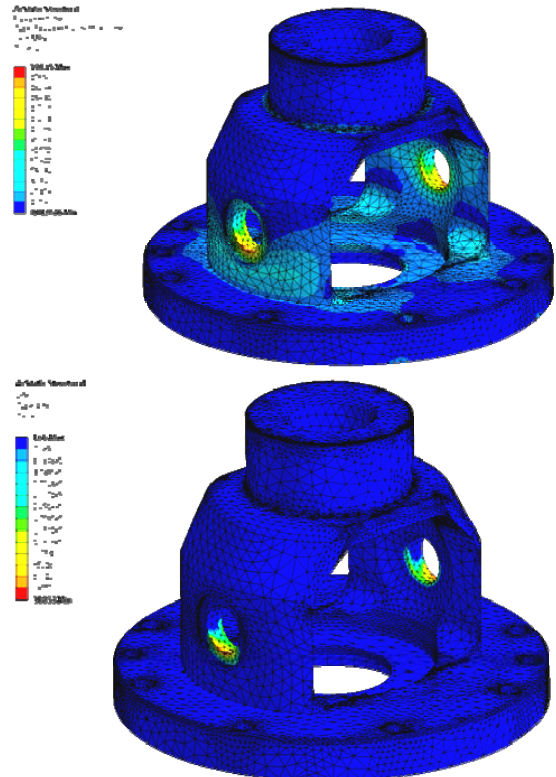


Fig. 13. Result of the stress and fatigue analyses on the differential case.

Finally, the disk housing was fixed on the bottom surface and the locking torque was applied on the top surface (Fig. 14).

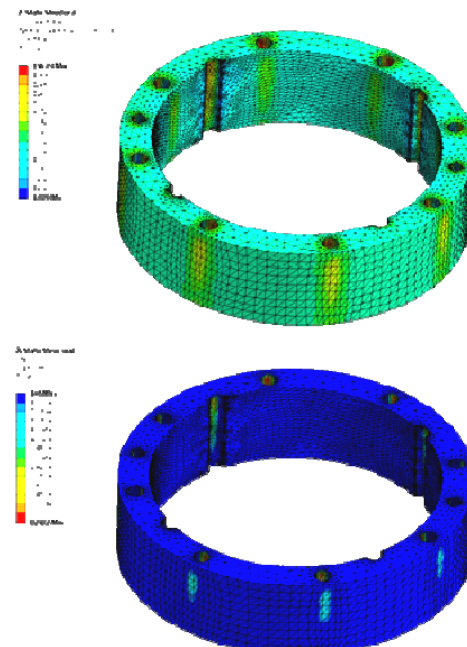


Fig. 14. Result of the stress and fatigue analyses on the disk housing.

The results of the stress analysis show that the yield limit was neither reached nor exceeded for all the components, according to the Von Mises criterion (Figures 12, 13, 14). Moreover, under the hypothesis of cyclic load, the fatigue life is fully acceptable [29]. Afterwards, a FEM analysis was carried out also on a three elements simplified assembly of the MRF LSD including the differential case, the disk housing and the differential gear. In particular, similar load conditions were applied and the necessary contact

constraints among these parts were defined. The analogous outcomes obtained were assumed adequate as the maximum stress results were significantly lower than the yield limit of the materials selected according to the Von Mises criterion. In Fig. 15 and Fig. 16 the results of the stress and fatigue analyses on the simplified assembly are showed.

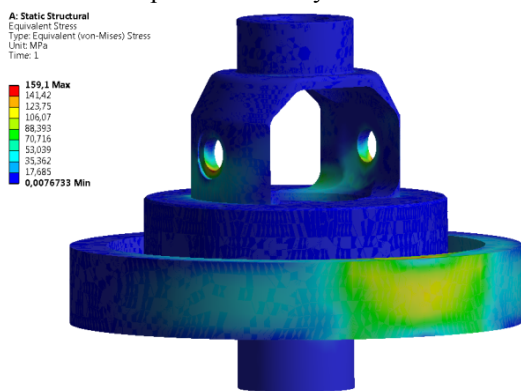


Fig. 15. Results of the stress analysis carried out on the simplified assembly of the MRF LSD.

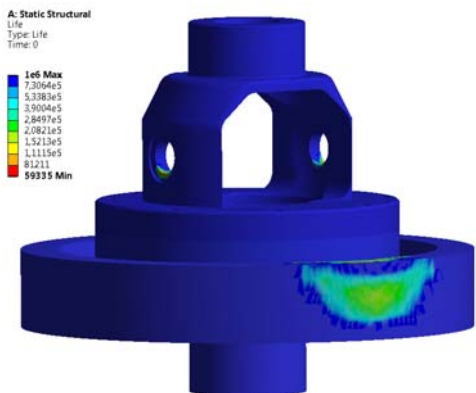


Fig. 16. Results of the fatigue analysis carried out on the simplified assembly of the MRF LSD.

Assembly procedures and GD&T

The GD&T is an essential tool to manufacture and to assemble parts. It allows to guarantee the functioning of the final product according to the requirements defined in the technical drawings taking into account the accuracy needed and the cost reduction [30]. So, the main parts of the MRF LSD had to be affected by specific geometric and dimensional tolerances to satisfy the functional requirements and to assure the best performances of the device.

The starting step was the identification of the datum elements to be used as main references for the assembly sequence of the parts of the MRF LSD and then the definition of the tolerances to be applied. The differential gear was the first element considered, due to its internal plane usable as base for the mating of the other parts of the MRF LSD. Then, two dowel pins were used as references to assemble the other elements. They allowed the displacement of the holes for the fastening operations and for the insertion of the disk housing MRF inside. This choice permitted to set very accurate tolerances for only two of the eight holes of the differential gear reducing the manufacturing costs. Then, the internal surfaces and the rotation axis were affected by adequate tolerances to avoid collisions between the differential gear and the coil housing that during the

functioning of the device is fixed. Particular attention was reserved to the rotor and stator disks and their spacers. Because of the partial contact between their surfaces, an accurate tolerance only for the contact areas was used to avoid unnecessary costs due to the machining phase. Lastly, because the gears are the main parts responsible for the correct motion transmission a suitable accuracy was used for it. Furthermore, a similar choice was adopted for the differential case because it had to be properly mated to the differential to avoid the spill of the MRF. The Fig. 17 shows the assembly sequence of the elements of the MRF LSD (Fig. 10) ideated starting from the DFA procedure. In particular, the differential gear is the first element to consider for the assembly phase. After the insertion of the dowel pins (1), the disk housing is mounted (2).

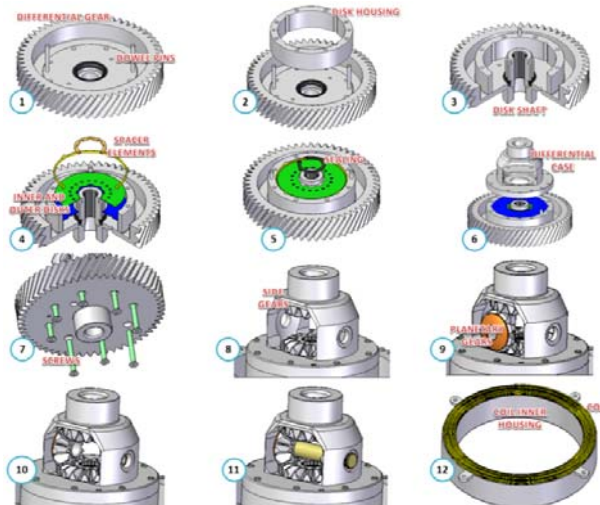


Fig. 17. CAD models of the parts of the MRF LSD and assembly sequence.

Then the disk shaft, the inner and the outer disks with the relative spacer elements are located (3 and 4). Afterwards the sealing and the differential case are positioned (5 and 6). The screws are used to tighten the disk housing and the disks subassembly, and to allow then the insertion of the MRF (7). Lastly, the gears and the coils are installed (8-12). Fig. 18 shows the first prototype of the MRF LSD manufactured by means of the typical CAM procedures. The differential gear was not completely refined because the teeth were not necessary for the testing process.



Fig. 18. Physical prototype of the MRF LSD.

V. TEST AND RESULTS

A test rig was set up in order to carry out the experimental investigations. It includes the MRF LSD, an inverter driven AC motor and a reduction unit. Suitable couplings were adopted to link the several components.

The measured quantities are:

- Rotational speed of the AC motor by phonic wheel and proximity pick up,
- Input current to the MRF LSD by Hall effect closed loop current sensor,
- Locking torque by high stiffness strain gauge load cell.

Current input was provided by an adjustable 3kW DC power supply. All measured quantities were acquired and stored by National Instruments Corporation board and software (LabVIEW ©).

The experimental test rig allows to measure the locking torque, i.e. the torque that engages the side gear A with the differential case P. With reference to Fig. 19, suitable bearings (A) sustain the differential case that was embedded in the load cell by means of rigid links (B). In this way, the locking torque is transmitted to the differential case, by means of the magnetic and the viscous effects, and its value is measured by the load cell. The coil housing (C) was fixed on a frame.

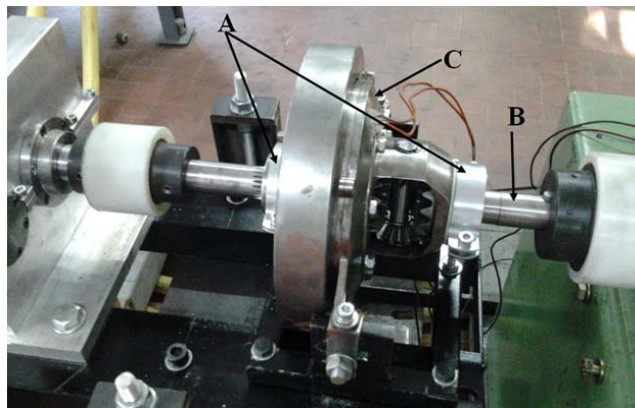


Fig. 19. MRF LSD on the test rig.

In order to evaluate the effectiveness of the manufactured MRF LSD, a result concerning the static torque-current relationship (Fig. 20) is presented. The test was conducted at a relative rotational velocity of 25 rpm. This constitutes a high value reachable in handling manoeuvres and consequently was functional to evaluate the viscous contribution on the locking torque. It can be observed that the MRF LSD is characterized by a limited zero current torque that makes the device similar to a common free differential. This allows to avoid not requested locking effects and undesirable vehicle dynamic behaviours [23]. At the same time, the MRF LSD exhibits a significant locking torque in presence of a reduced supply current and shows a substantially linear tendency that allows an easier feedback controller design procedure [10, 11, 31].

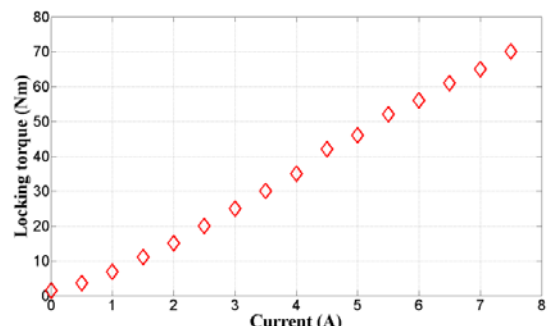


Fig. 20. Locking torque vs supply current.

The transient response of the device was obtained adopting as input an up-step down-step sequence in terms of supply current with an amplitude of 7 A. Fig. 21 shows the output torque of the MRF LSD normalized by the respective maximum value. The input-output relationship can be well approximated by a first order linear time-invariant system and consequently a 63.2% time constant of 0.03 s was determined, satisfying the typical dynamic requirements of the vehicle handling control systems.

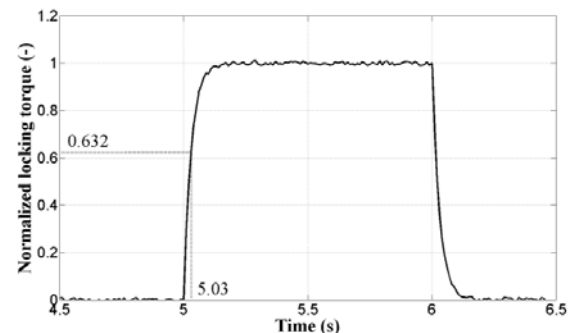


Fig. 21. Step response of the MRF LSD.

Fig. 22 illustrates the locking torque in presence of a sine law employed for the supply current. Particularly, the input is characterized by both the mean value and the amplitude of 1 A, while the frequency is 1 Hz.

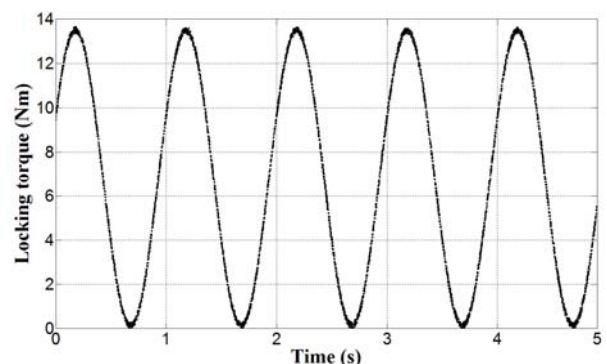


Fig. 22. Response to a sine input.

The static and dynamic properties illustrated above allow to observe:

- a value of locking torque fully enough to control the yaw moment in a vehicle;
- a requested current fully available on a common vehicle;
- a time constant of the device that highlights a fast engagement;
- the absence of hysteresis and residual magnetization.

VI. CONCLUSIONS

An automotive magnetorheological semi-active differential was designed starting from a Reverse Engineering process on a common gearbox that was equipped in origin with a free differential, defining the most challenging geometrical constraints of the new device. The first result of this procedure was to get the CAD model of the differential housing reconstructed by means of a complex feature recognition phase. Furthermore, it allowed to individuate the available volume and to reach the second target defined at the beginning i.e. the design of the first virtual prototype of the MRF LSD by means of a preliminary CAD modeling phase. As final result, the optimization of the dimensions, realized according to the proper choice of the materials, determined the final CAD model allowing the manufacturing of the physical prototype too.

Finally, the tests demonstrated the validity of the design process and the goodness of the simulations done. Indeed, the torque-current relationship showed the inclination of the MRF LSD to be a useful tool to control the yaw moment and, consequently, to improve the vehicle handling.

ACKNOWLEDGMENT

The authors deeply thank the engineers Antonio Aletta, Roberto Conte, Vito Rufrano and Rosario Salemme for their indispensable technical support.

REFERENCES

- [1] J. Cecil, A. Kanchanapiboon, "Virtual engineering approaches in product and process design", in *The International Journal of Advanced Manufacturing Technology*, 2007, 31 (9): 846-856.
- [2] G. Sun, W. Ren, J. Zhang, "Virtual product development for an automotive universal joint", *International Journal of Automotive Technology*, Vol. 12, No. 2, pp. 299–305 (2011), DOI 10.1007/s12239-011-0035-7.
- [3] G. Di Gironimo, A. Lanzotti, "Designing in VR", *Int J Interact Des Manuf* (2009) 3:51–53, DOI 10.1007/s12008-009-0068-6.
- [4] B. Furt (Ed.), "Handbook of Augmented Reality", Springer-Verlag New York Inc ©, XXII, ISBN: 978-1-4614-0063-9, (2011).
- [5] D. Michalak, "Applying the Augmented Reality and RFID Technologies in the Maintenance of Mining Machines", Lecture Notes in Engineering and Computer Science: Proceedings of the World Congress on Engineering and Computer Science 2012, WCECS 2012, 24-26 October, 2012, San Francisco, USA, pp. 256 - 260.
- [6] G. Di Gironimo, C. Labate, F. Renno, G. Broletti, F. Crescenzi, F. Crisanti, A. Lanzotti, F. Lucca, "Concept Design of Divertor Remote Handling System for the FAST Machine", *International Journal on Interactive Design and Manufacturing* 3 (2), pp. 65-79, Article in Press, 2013.
- [7] A. Raneda, P. Pessi, M. Siuko, H. Handroos, J. Palmer, M. Vilenius, "Utilization of virtual prototyping in development of CMM", *Fusion Engineering and Design* 69 (2003) 183-186.
- [8] G. Ramogida, G. Calabro, V. Coccilovo, F. Crescenzi, F. Crisanti, A. Cucchiaro, G. Di Gironimo, R. Fresa, V. Fusco, P. Martin, S. Mastrotostefano, R. Mozzillo, F. Nuzzolese, F. Renno, C. Rita, F. Villone, G. Vlad, "Active toroidal field ripple compensation and MHD feedback control coils in FAST", *Fusion Engineering and Design* 88 (6-8), pp. 1156-1160, 2013.
- [9] L. Golebiowski, D. Mazur, "Analysis and Simulation of Electrical and Computer Systems", Springer, 2014. ISBN-13: 978-3319112473.
- [10] A. Lanzotti, F. Renno, M. Russo, R. Russo, M. Terzo, "Design and development of an automotive magnetorheological semi-active differential", *Mechatronics*, vol. 24, no. 5, pp. 426 – 435, 2014.
- [11] A. Lanzotti, F. Renno, M. Russo, R. Russo, M. Terzo, "A physical prototype of an automotive magnetorheological differential", *Lecture Notes in Engineering and Computer Science*, vol. 3 LNECS, pp. 2131 – 2135, 2013.
- [12] R. Durairaj, L.W. Man, L.J. Ping, L.S. Pheng, and R.T. Subramaniam, "Rheology and Processability of Diglycidylether of bisphenol-A (DGEBA) and Polyurethane (PU) based Isotropic Conductive Adhesives Filled with Different Size-distributed Silver Flakes and Silver Particles", *Engineering Letters*, vol. 21, no.:3, pp.143-148, 2013.
- [13] V. Raja, K.J. Fernandes, "Reverse Engineering, An Industrial Perspective". *Springer Series in Advanced Manufacturing*. Springer-Verlag London, 2008.
- [14] A.C. Telea, "Reverse Engineering - Recent Advances and Applications", Ed. Intech 2012, ISBN 978-953-51-0158-1.
- [15] K. Karakoc, E.J. Park, A. Suleman, "Design considerations for an automotive magnetorheological brake", *Mechatronics* 2008; 18: 434-447.
- [16] B. Kavlicoglu, N. Kavlicoglu, Y. Liu, C. Evrensel, A. Fuchs, G. Korol and F. Gordanejad., "Response time and performance of a high-torque magneto-rheological fluid limited slip differential clutch", *Smart Materials and Structures*, vol. 16, pp. 149-159, 2007.
- [17] G.Z Yao, F.F. Yap, G. Chen, W.H. Li, S.H. Yeo, "MR damper and its application for semi-active control of vehicle suspension system", *Mechatronics*, vol. 12, pp. 963 – 973, 2002.
- [18] I.H. Taureg, J. Horst, "Induced torque amplification in viscous couplings", SAE Paper 900557 1990.
- [19] J. An, D.S. Kwon, "Modeling of a magnetorheological actuator including magnetic hysteresis", *J Intel Mater Syst Struct*, vol. 14, no. 9, pp. 541–50, 2003.
- [20] R. Russo, M. Terzo, "Modeling, parameter identification, and control of a shear mode magnetorheological device", *Proc IMechE Part I: Journal of Systems and Control Engineering*, vol. 225, no. 5, pp. 549 – 562, 2011.
- [21] R. Russo, M. Terzo, "Design of an adaptive control for a magnetorheological fluid brake with model parameters depending on temperature and speed", *Smart Materials and Structures*, vol. 20, no. 11, 115003 (9pp), 2011.
- [22] M. Terzo, "Employment of magneto-rheological semi-active differential in a front wheel drive vehicle: Device modelling and software simulations", *SAE Technical Papers* 2009-24-0130, doi:10.4271/2009-24-0130, 2009.
- [23] R. De Rosa, M. Russo, R. Russo, M. Terzo, "Optimisation of Handling and Traction in a Rear Wheel Drive Vehicle by Means of Magneto-Rheological Semi-Active Differential", *Vehicle System Dynamics*, vol. 47, no. 5, pp. 533 – 550, 2009.
- [24] The Joint Laboratory "Interactive DEsign And Simulation" <http://www.ideas.unina.it/>.
- [25] G. Di Gironimo, A. Lanzotti, K. Melemez, F. Renno, "A top-down approach for virtual redesign and ergonomic optimization of an agricultural tractor's driver cab", *Proceedings of the ASME 2012 11th Biennial Conference On Engineering Systems Design And Analysis ESDA2012*, July 2-4, 2012, Nantes, France.
- [26] D. E. Whitney, "Mechanical Assemblies: Their Design, Manufacture, and Role in Product Development", Oxford University Press, ISBN: 9780195157826, 2004.
- [27] ANSI-AGMA 2005-C96. "Design manual for bevel gears". American Gear Manufacturers Association, 1988.
- [28] ANSI-AGMA-ISO 6336-6-A08. "Calculation of load capacity of spur and helical gears – part 6: calculation of service life under variable load". American Gear Manufacturers Association, 2008.
- [29] R.C. Rice, B.N. Leis, H.D. Berns, D.V. Nelson, D. Lingenfleser, M.R. Mitchell, "Fatigue design handbook". SAE, Warrendale; 1988.
- [30] G. Henzold, "Geometrical Dimensioning and Tolerancing for Design", Manufacturing and Inspection, Elsevier Ltd., 2006, ISBN: 978-0-7506-6738-8.
- [31] S. Strano, M. Terzo, "A first order model based control of a hydraulic seismic isolator test rig", *Engineering Letters*, vol. 21, no. 2, pp. 52 – 60, 2013.